Turkish Journal of Electrical Engineering & Computer Sciences

http://journals.tubitak.gov.tr/elektrik/

Research Article

Turk J Elec Eng & Comp Sci
(2024) 32: 108 – 125

doi:10.55730/1300-0632.4058

Fractional delay-dependent load frequency controller design for a single-area power system with communication delay

Erhan YUMUK[1,2*]

[1]Department of Control and Automation Engineering, Electrical Electronics Faculty, İstanbul Technical University, İstanbul, Turkiye

[2]Department of Electromechanics, System and Metal Engineering, Ghent University, Ghent, Belgium

Received: 27.08.2023 • **Accepted/Published Online:** 05.01.2024 • **Final Version:** 07.02.2024

Abstract: This paper proposes a fractional delay-dependent load frequency control design approach for a single-area power system with communication delay based on gain and phase margin specifications. In this approach, the closed-loop reference transfer function relies on the delayed Bode's transfer function. The gain and phase margin specifications are established in order to optimize the reference model based on three time-domain performance indices. Here, a category of fractional-order model is employed to describe the single-area power system incorporating communication delay. The controller parameters are determined using the fractional-order system model and optimal closed-loop reference model. Then, a delay-dependent control mechanism is proposed to compensate for the communication delay variations. The proposed controllers are implemented in a single area power system with nonreheated turbine having communication delay and are compared with other controllers designed relying on identical frequency domain specifications. The performance analysis of the proposed approach is made against communication delay variations, model parameter variations, and nonlinearities, i.e. governer dead band and governor rate constraints. Furthermore, the scope of the analysis extends beyond a single-area power system to encompass a multi-area power system, illustrating the effectiveness of the proposed method. The outcomes demonstrate that the performance of the proposed controllers surpasses that of alternative control methods, they are more robust to communication delay changes as well as system model parameter variations, and they perform efficiently in the case of multiarea case study.

Key words: Fractional delay-dependent, load frequency controller, delayed Bode's transfer function, power systems with nonreheated turbine, single fractional order pole model, gain and phase margin specifications

1. Introduction

Load frequency control (LFC) has seen significant interest and has become a focal point of interest for researchers in the field of power system engineering. The role of LFC in Power Systems (PS) is to regulate the frequency to a predetermined nominal value in the event of power fluctuations. The main concerns in designing a LFC system are (i) to achieve zero steady-state error when there is a frequency deviation, (ii) to maintain a satisfactory load disturbance rejection performance, (iii) to ensure robustness against modeling uncertainties and system nonlinearities, and (iv) to minimize line power flow between neighboring areas in case of multi-area PS. There exist numerous studies dealing with these problems on PS [1–3]. On the other hand, another challenge associated with LFC is time delays due to various factors such as power line carriers, phasor measurement units, and remote

*Correspondence: yumuk@itu.edu.tr

terminal units transmitting data to a local control center. Although these communication delays can degrade the control system performance, there exist few studies dealing with this problem in PS [4–6].

Power systems (PS) possess various subsystems such as the governor, turbine, load, machine, etc. Since each subsystem can be described by the first-order transfer function, a higher-order differential equation is required to express all the PS dynamics. However, LFC design for this category of systems is a challenging endeavor. Therefore, the higher-order differential equation is generally reduced by simple integer order system models [1, 2]. LFC designed using these reduced integer-order models can have insufficient performance because of modeling errors and system nonlinearities. In general, recent studies show that fractional-order models represent the system dynamics better compared to integer-order models [7]. As far as the author is aware, there do not exist any fractional-order models for the representation of PS. For this aim, the fractional order equivalent of the first order plus time delay (FOPTD) model is chosen, which is referred to as single fractional order pole model (SFOPM) [7].

There are various LFC design methods in literature: (i) Classical approaches such as PID control, internal model control, and cascaded control [1]; (ii) Advanced approaches such as fractional control [8], adaptive control [9], etc. In spite of so numerous advanced strategies available in the literature, the most extensively used LFC strategy is PID control in the diverse field of control engineering. Gain and Phase Margin (GPM) specifications are selected to design a robust PID controller against modeling error and system nonlinearities [5]. Moreover, fractional order controller design in PS has attracted many researchers since it offers a convenient design methodology in the frequency domain. The most prominent strategy is fractional order PID (FOPID) control, which is a generalized form of integer order PID control [10]. Regarding this matter, Bode shaping stands out as one of the most powerful frameworks in the context of designing fractional-order controllers using frequency-based methods. This framework allows the ability to analytically design fractional controllers. Among the frequently employed frequency domain specifications, GPM are commonly employed as indicators of robustness in PS. Utilizing the specifications, some revised Bode's transfer functions are proposed for the development of robust analytical fractional-order PID controllers [11]. Moreover, Bode shaping is used to design load frequency controller [10]. Nevertheless, these controllers do not perform satisfactorily in achieving the desired frequency domain specifications when the system includes a time delay. Consequently, the delayed Bode's transfer function is brought into consideration [12]. By employing this transfer function, the performance of the control system has been enhanced for time-delay systems in terms of GPM specifications in [8]. Despite these frequency-based fractional controller design, these frequency domain specifications do not offer immediate insight into time domain criteria, which are essential aspects of the control system design. Consequently, a novel approach to fractional-order controller design, which relies on the choice of optimal frequency-domain specifications, has been introduced for time delay systems in [13].

In this study, a fractional delay-dependent LFC design approach for a single-area Power System with NonReheated Turbine (PS-NRT) having communication delay is proposed. In this approach, GPMs are used as the design specifications, and the closed-loop reference transfer function relies on the delayed Bode's transfer function. The GPM specifications are subsequently defined in order to optimize the reference model based on three different time-domain performance indices. Then, the single-area PS-NRT with communication delay is represented by a class of fractional-order model. The parameters of the controller are found employing the fractional-order system model and optimal closed-loop reference model. Finally, a fractional delay-dependent control mechanism is designed to compensate for the communication delay variations. The controllers proposed

in the paper are implemented in a single-area PS-NRT having communication delay, and are compared with other controllers designed relying on the identical frequency domain specifications. The performance analysis of the proposed approach is made against communication delay or model parameter variations, and nonlinearities, i.e. governer dead band and governor rate constraints. Furthermore, the scope of the analysis extends beyond a single-area power system to encompass a multi-area power system, illustrating the effectiveness of the proposed method. The outcomes demonstrate that the performance of the proposed controllers surpasses that of alternative control methods, they are more robust to communication delay changes as well as system model parameter variations, and they perform efficiently in the case of multi-area case study.

The key contributions of the paper may be outlined as follows: (i) A fractional-order model of a single area PS-NRT having communication delay is obtained, (ii) The optimal delayed Bode's transfer function is used to design load frequency controller, (iii) A fractional delay-dependent controller is proposed using an optimal transfer function and (iv) The efficiency of the proposed controller is illustrated on a single area PS-NRT having communication delay.

The paper is structured in the following manner: A single area PS-NRT having communication delay is introduced and a fractional-order model is extracted in Section 2. In Section 3, a fractional delay-dependent LFC design method is proposed using an optimal unity feedback reference system. Section 4 offers a performance analysis to show the efficiency of the proposed design approach. Finally, Section 5 is devoted to the discussion and conclusion.

2. Single area load frequency control system

Even though a single area PS possesses a highly nonlinear characteristic, its linearized model can be obtained subject to small load changes in an operating condition. The purpose of the PS is to regulate the frequency deviation (Δf) against the load disturbance deviation (ΔP_d). Figure 1 illustrates the block diagram of a single area LFC system which consists of a load frequency controller ($C(s)$) and a single area PS with communication delay ($G(s)$).

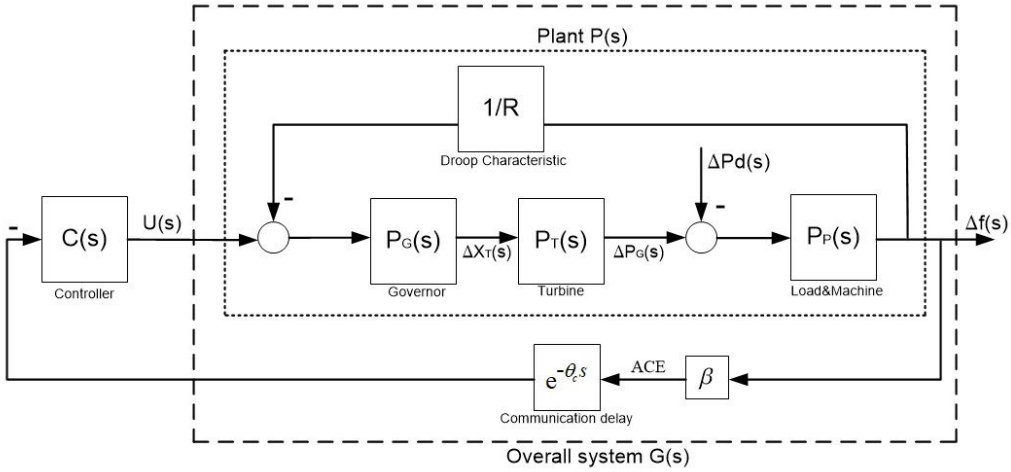

Figure 1. The block diagram of a single area LFC system.

2.1. Dynamics of single area power system with nonreheated turbine

There exist three subsystems in a single area PS-NRT as shown in Figure **??**: Governor ($P_G(s)$), Turbine ($P_T(s)$), and Load and machine ($P_P(s)$) In this study, we consider nonreheated turbine with droop characteristics. These three subsystems are given in the following model forms:

$$P_G(s) = \frac{1}{sT_G + 1} \tag{1}$$

$$P_T(s) = \frac{1}{sT_T + 1} \tag{2}$$

$$P_P(s) = \frac{1}{Ms + D} \tag{3}$$

where T_G and T_T are the governor and turbine time constants, respectively. M and D denote inertia constant and damping coefficient, respectively. The dynamics of the single area PS-NRT which will be considered as plant $P(s)$ can be found as

$$P(s) = \frac{P_G(s)P_T(s)P_P(s)}{1 + P_G(s)P_T(s)P_P(s)/R} \tag{4}$$

Here, R denotes the droop characteristics of a nonreheated turbine. The dynamics of the single area PS-NRT having communication delay which is represented as $G(s)$ in Figure 1 is found as

$$G(s) = \beta P(s)e^{-\theta_c s} \tag{5}$$

where β and θ_c are frequency bias constant and communication delay. In this study, the parameters of PS are taken as $T_G = 0.1, T_T = 0.3, M = 10, D = 1, R = 0.05, \beta = 21$, and $\theta_c = 2.28$. The reason for selecting these parameters is that they have been utilized in various related applications of PS [4, 6**?**]. As a result, the following higher-order transfer function model of PS-NRT and the overall system is calculated using Eqs. (4) and (5), respectively:

$$P(s) = \frac{3.33}{s^3 + 13.43s^2 + 34.67s + 70.00} \tag{6}$$

$$G(s) = \frac{70.00}{s^3 + 13.43s^2 + 34.67s + 70.00}e^{-2.28s} \tag{7}$$

2.2. Fractional order model of single area power system with nonreheated turbine having communication delay

Power systems possess extremely interconnected networks. Even the order of a simple single area PS is three. The higher-order differential equation is generally reduced by the integer reduced order system models, i.e. FOPTD models [1, 2]. Load frequency controllers designed using these models can have insufficient performance because of modeling error and system nonlinearities. However, it is a well-known fact that higher-order dynamics may be represented by fractional-order models with fewer parameters [7]. The fractional order equivalent of the FOPTD model which is referred to as the Single Fractional Order Pole Model(SFOPM) is chosen in this study. The transfer function is as follows:

$$P_{SFOPM}(s) = \frac{K_s}{T_s s^{\alpha_s} + 1}e^{-\theta_s s} \tag{8}$$

where K_s, T_s, $\alpha_s \in (0,2)$ and θ_s denote the gain, time constant, fractional order, and time delay of the model, respectively. This model is the simplest fractional order time delay model since it is acquired by introducing a fractional order into the integer FOPTD model. In this study, the dynamics of PS are represented by a fractional order model for the first time in the literature.

Oustaloup filter approximation is employed to implement the fractional operators in both fractional order models in (8) and controllers to be designed. This filter approximation for the fractional operator with the order $\alpha \in (0,1)$ might be given by

$$s^\alpha = O(s^\alpha) = K' \prod_{k=1}^{N} \frac{s+\omega'_k}{s+\omega_k} \tag{9}$$

where

$$K' = \omega_h^\alpha, \quad \omega'_k = \omega_l \left(\frac{\omega_h}{\omega_l}\right)^{\frac{2k-1-\alpha}{2N}} \quad \omega_k = \omega_l \left(\frac{\omega_h}{\omega_l}\right)^{\frac{2k-1+\alpha}{2N}}$$

Moreover, N is the order of the filter, the upper and lower frequency bounds in the filter are denoted by ω_h and ω_l, respectively. These parameters are selected as $N = 11, \omega_h = 10^3, \omega_l = 10^{-3}$ [12].

Fractional order model identification poses a highly nonlinear optimization problem due to its dependence on a number of pole-zero pairs. Genetic Algorithm (GA) is a widely recognized global optimization approach to address such complexity. Moreover, GA demonstrates proficiency in addressing complex problems and leveraging parallelism, effectively managing diverse optimization scenarios. Despite of some parameter tuning, including fitness function, population size, mutation, and crossover rates etc., GAs are extensively employed in modern nonlinear optimization for fractional order models [14, 15]. Therefore, GA is employed to find SFOPM parameters of PS-NRT, i.e. $K_s, T_s, \alpha_s, \theta_s$ by minimizing the least square error. Finally, the SFOPM parameters are obtained as

$$K_s = 0.047, T_s = 0.31, \alpha_s = 1.32, \theta_s = 0.25 \tag{10}$$

For a comparison purpose, the dynamics of the PS-NRT can be modelled by a second reduced-order transfer function using Routh approximation model reduction scheme. The second reduced-order model is derived in the following manner:

$$P_{Routh}(s) = \frac{0.29}{s^2 + 3.04s + 6.13} \tag{11}$$

The step responses of PS-NRT and corresponding models in (8) and (11) are shown in Figure 2a. The modeling errors of the Routh model and SFOPM are found as 1.252×10^{-9} and 8.235×10^{-10}, respectively. It can be confidently asserted that a fractional-order model provides a more accurate representation of PS dynamics. Moreover, the frequency responses of the PS-NRT and the reduced order models in (8) and (11) are illustrated in Figure 2b. It can be readily asserted that the frequency response of SFOPM also closely approximates that of the power system.

Finally, we can obtain the following models for the PS-NRT having communication delay using Eq. (**??**) for both the Routh model and SFOPM:

$$G_{Routh}(s) = \beta P_{Routh}(s) e^{-\theta_c s} = \frac{6.13}{s^2 + 3.04s + 6.13} e^{-2.28s} \tag{12a}$$

$$G_{SFOM}(s) = \beta P_{SFOM}(s) e^{-\theta_c s} = \frac{0.99}{0.31 s^{1.32} + 1} e^{-2.53s} \tag{12b}$$

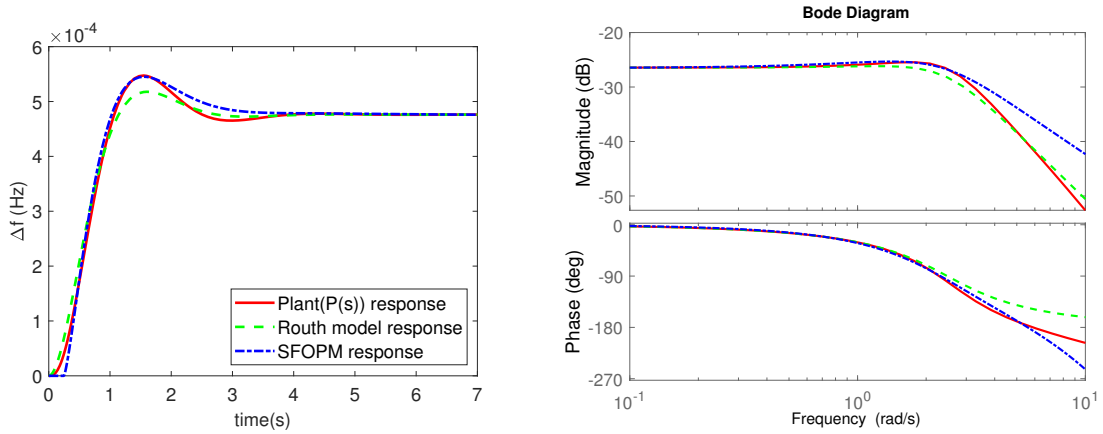

(a) **(b)**

Figure 2. (a) Step responses and (b)Frequency responses of PS-NRT and the reduced order models

3. Design of fractional delay-dependent load frequency controller

3.1. Delayed Bode's transfer function

Bode's transfer function (BTF) is given as:

$$L(s) = \frac{K_d}{s^\gamma} \tag{13}$$

where $K_d, \gamma \in R$ are the gain and fractional order of BTF, respectively. BTF for $\gamma > 0$ and $\gamma < 0$ represents fractional integration and differentiation, correspondingly. The amplitude curve slope is -20γ dB/dec on the logarithmic axis, and the phase curve remains at a value of $-\pi\gamma/2$ rad throughout all the frequencies. Moreover, the delayed Bode's transfer function (D_BTF) proposed in [12] is given as

$$L(s) = \frac{K_d}{s^\gamma} e^{-\theta s} \tag{14}$$

where θ is the time delay. The amplitude curve slope is similar to in BTF. However, the phase curve of D_BTF has a value of $-\pi\gamma/2 - \omega\theta$ rad. Unlike BTF case, the phase curve is dependent on frequency ω.

In controller design for fractional order systems, a reference model can be selected, such as in the integer case, and the behavior of the control system is desired to be as close to the reference model as possible. In this study, the delayed Bode transfer function with unit feedback is chosen as the reference model. For this purpose, the transfer functions of the reference model and the control system are equalized with the direct synthesis method and a fractional order controller is designed.

3.2. Controller structure

The unity feedback control system in which $L(s)$ is positioned in the feedforward path is considered as it is depicted in Figure 3a. The reference transfer function for the closed-loop system is defined as follows:

$$T_{ref}(s) = \frac{L(s)}{1 + L(s)}. \tag{15}$$

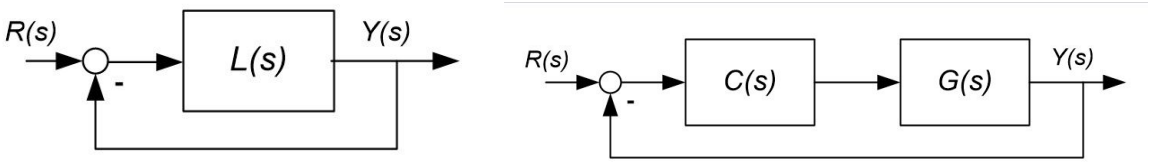

(a) **(b)**

Figure 3. Block diagrams of (a) reference model with D_BTF and (b) the unity feedback control system.

A unity feedback control system whose block diagram is illustrated in Figure 3b is going to be employed in the design methodology. Here, $G(s)$ and $C(s)$ are the system model and controller whereas $Y(s)$ and $R(s)$ denote output and reference signals, respectively. In this study, the system model $G(s)$ is accepted as $SFOPM$.

The GPM specifications that the controller in Figure 3b needs to satisfy are regarded as

- Gain Margin: $|C(j\omega_p)G(j\omega_p)| = \frac{1}{A_m}$, where ω_p is phase crossover frequency.
- Phase Margin: $\angle C(j\omega_g)G(j\omega_g) = \phi_m - \pi$, where ω_g is gain crossover frequency.

When D_BTF is employed as the reference transfer function, the controller in Figure 3b might be designed such that the desired GPM specifications are satisfied. Next, by setting θ equal to the time delay of the system model in (8) and by inverting the minimum phase component of the system model in (8), the controller is formulated as

$$C(s) = \frac{K_d(T_s s^{\alpha_s} + 1)}{K_b s^{\gamma}} \tag{16}$$

This controller can also be represented in filtered fractional order PI form:

$$C(s) = \frac{K_d T_s}{K_s} s^{\alpha_s - \gamma} \left(1 + \frac{1}{T_s s^{\alpha_s}}\right) \tag{17}$$

Here, K_s, T_s and α_s are the model parameters in (8). For the fractional order LFC design, it is necessary to calculate K_d and γ that meet the desired GPM specifications ϕ_m, A_m. Therefore, the frequency response of D_BTF in (14) is given as

$$L(j\omega) = \frac{K_d}{(j\omega)^{\gamma}} e^{-j\omega\theta} \tag{18}$$

$$= \frac{K_d}{(\omega)^{\gamma}} e^{-j\left(\omega\theta + \frac{\gamma\pi}{2}\right)} \tag{19}$$

The magnitude and phase functions of D_BTF are parametrically calculated as

$$|L(j\omega)| = \frac{K_d}{(\omega)^{\gamma}} \tag{20}$$

$$\angle L(j\omega) = -\omega\theta - \frac{\gamma\pi}{2} \tag{21}$$

For D_BTF to meet the desired phase margin(ϕ_m) specification, it is essential to solve the following two nonlinear equations:

$$|L(j\omega_g)| = 1 \quad \Rightarrow \quad K_d = \omega_g^{\gamma} \tag{22a}$$

$$\angle L(j\omega_g) = \phi_m - \pi \quad \Rightarrow \quad \frac{-\gamma\pi}{2} = -\pi + \phi_m + \omega_g\theta \tag{22b}$$

Likewise, for D_BTF to meet the desired gain margin(A_m) specification, it is necessary to solve the following two nonlinear equations:

$$\angle L(j\omega_p) = -\pi \quad \Rightarrow \quad \frac{-\gamma\pi}{2} = -\pi + \omega_p\theta \tag{23a}$$

$$|L(j\omega_p)| = \frac{1}{A_m} \quad \Rightarrow \quad K_d = \frac{\omega_p^{\gamma}}{A_m} \tag{23b}$$

Lastly, the four nonlinear equations with four unknown variables, K_d, γ, ω_g and ω_p are obtained. When these four nonlinear equations are solved employing fixed point iteration method D_BTF parameters, K_d and γ are found. Then, the parameters of the fractional order controller in (**??**) are calculated.

These frequency domain specifications do not offer immediate insight into time domain criteria, which are essential aspects of the control system design. Hence, it is possible to consider time domain criteria when establishing frequency domain specifications.

3.3. Stability evaluation of the reference model

The stability of a unity feedback reference model with a forward path incorporating Bode's transfer function relies on Matignon's Theorem, formally referred to as Theorem 1. The proof for this theorem can be located in [10].

Theorem 1 *For a fractional order system with the characteristic equation given as*

$$P(s) = \sum_{i=0}^{k} a_i s^{i\gamma},$$

the system is bounded input-bounded output stable if and only if the following conditions are met:

$$0 < \gamma < 2, \quad |\angle \upsilon_k| > \frac{\gamma\pi}{2}, (k = 1, 2, ..., n)$$

where υ_k *are the roots of polynomial* $P(\upsilon) = \sum_{i=0}^{k} a_i \upsilon^i$.

In the scenario of the delayed Bode's transfer function, there is a transcendental characteristic equation with a fractional order. The stability criteria for the reference model used in this study is detailed in Theorem 2, and the proof for this theorem can be located in [13].

Theorem 2 *The necessary and sufficient condition for bounded input-bounded output stability of the delayed Bode transfer function with unity feedback is given as*

$$\left(\frac{\pi - \frac{\pi\gamma}{2}}{\theta}\right)^{\gamma} \frac{1}{K_d} > 1$$

As indicated by Theorem 2, the stability area for the reference model is visually represented in Figure 4.

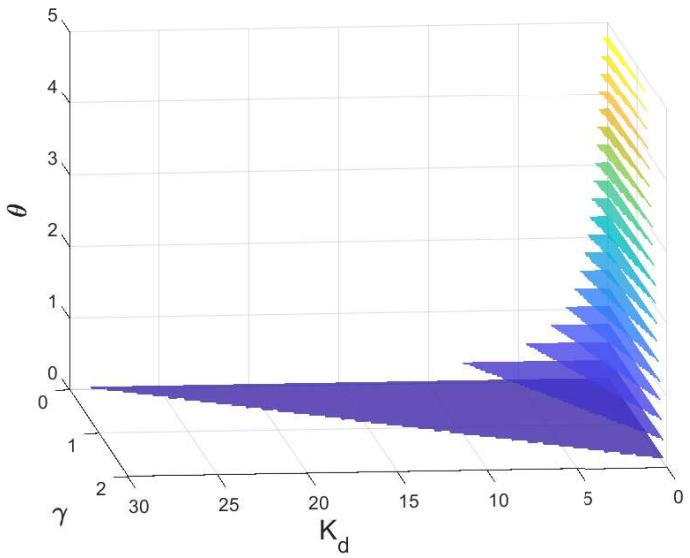

Figure 4. Stability area of the reference model

3.4. A optimal strategy to select frequency-domain specifications utilizing time domain criteria

In [13], the selection strategy of GPM specifications in D_BTF is proposed based on the following three time domain criteria; namely, Integral Square Error (ISE), Integral Absolute Error (IAE), and Integral Time Square Error (ITSE):

$$ISE = \int_{t=0}^{t=\infty} e^2(t)dt \tag{24a}$$

$$IAE = \int_{t=0}^{t=\infty} |e(t)|dt \tag{24b}$$

$$ITSE = \int_{t=0}^{t=\infty} te^2(t)dt \tag{24c}$$

Here, $e(t)$, which corresponds to the discrepancy between reference $r(t)$ and output $y(t)$ signals, denotes the error signal.

In Section 3.2, it is explained that the delay term of D_BTF is set to be identical to the time delay of the model. The other parameters, γ, K_d of D_BTF may then be found using time domain criteria. For this aim, these parameters are found for each time delay value within the range of (0, 5] according to ISE, IAE, and ITSE. A genetic algorithm is employed to find the optimal parameters, and their variations in terms of time delay value are shown in Figures 5a and 5b. It appears from these figures that the optimal values of the fractional order γ of D_BTF slightly depend on the time delay (it is almost a constant value). Nevertheless, the optimal gain values, denoted as K_d, exhibit an inverse relationship with the time delay θ.

Next, the corresponding GPM values are calculated for each optimal D_BTF using Eqs. 22a, 22b, 23a, and 23b. These values are illustrated in Figures. 5c and 5d. It is clearly seen from these figures that the GPM values slightly depend on the time delay similar to the optimal gain K_d.

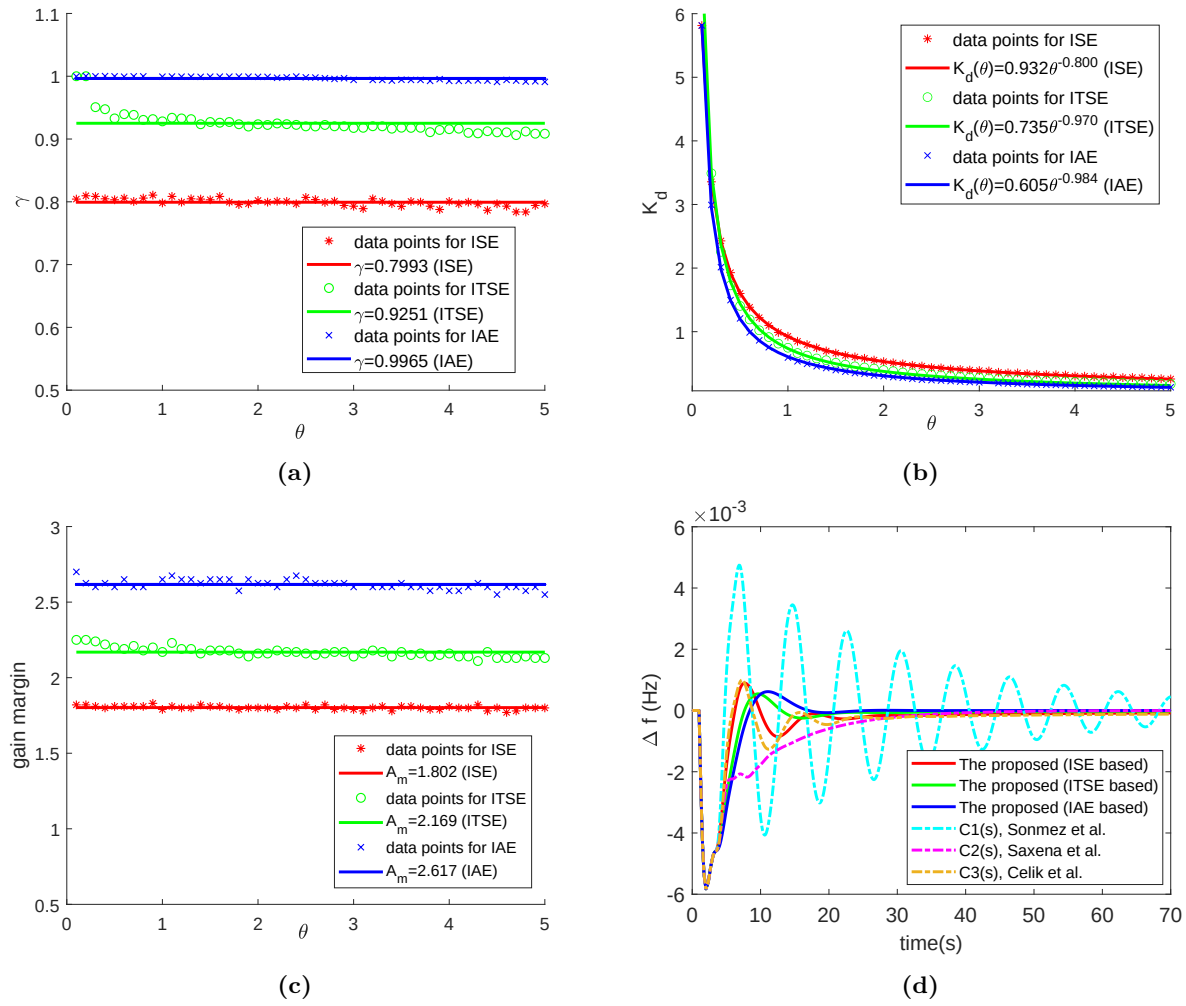

Figure 5. (a) The optimal γ values, (b) The optimal K_d values, (c) The gain margin values and (d) The phase margin values of the optimal delayed BTF.

The approximating functions of these frequency domain specifications, PM and GM for each time domain criterion can be obtained using MATLAB Curve Fitting Toolbox. Moreover, the approximating functions are also fitted for K_d and γ in a similar way. These functions are given in Table 1. Furthermore, these functions are illustrated in Figures 5a, 5b, 5c, and 5d.

When the communication delay of PS is known, the D_BTF parameters, K_d and γ are found using the equations given in Table 1. Then, the fractional-order controller is designed using Eq. (**??**). However, the designed controller has an insufficient performance when the communication delay is unknown or changed. In this case, it would be better to design a controller whose parameters are changed according to communication delay.

Table 1. Approximating functions for frequency-domain specifications and the D_BTF parameters.

Performance index	$PM(\theta)$	$GM(\theta)$	$\gamma(\theta)$	$K_d(\theta)$
ISE	56.330	1.802	0.799	$0.932\theta^{-0.800}$
ITSE	54.840	2.169	0.925	$0.735\theta^{-0.970}$
IAE	55.910	2.617	0.996	$0.605\theta^{-0.984}$

3.5. Fractional delay-dependent controller design

As it can be illustrated in Figures 5a and 5b, the optimal D_BTF parameters are time delay-dependent. Therefore, the controller in (**??**) can be presented in terms of time delay as follows:

$$C(s,\theta) = \frac{K_d(\theta)T_s}{K_s} s^{\alpha_s - \gamma(\theta)} \left(1 + \frac{1}{T_s s^{\alpha_s}}\right) \tag{25}$$

Here, the derived functions in Table 1 are used for $K_d(\theta)$ and $\gamma(\theta)$. θ consists of communication delay (θ_c) and the delay (θ_s) induced by higher order dynamics of PS as follows:

$$\theta = \theta_c + \theta_s \tag{26}$$

The control structure offers the possibility to adapt LFC design against the changes in the communication delay. For the single area PS-NRT mentioned in this study, the delay (θ_s) induced by its higher order dynamics is equal to 0.25 s given in Eq. (10)

The principle of the proposed delay-dependent LFC design methodology can be summarized as the following simple procedure:

i. Obtain the parameters of the fractional order model in (8) of the single area PS, i.e. K_s, T_s, α_s, and θ_s using genetic algorithm.
ii. Find optimal D_BTF parameters, K_d, γ for each θ values according to ISE, IAE and ITSE criteria (See Figures 5a and 5b).
iii. Calculate the corresponding GPMs for each optimal value parameter set using Eqs. (22a)-(23b) (See Figures 5c and 5d)
iv. Find the optimal D_BTF parameters $K_d(\theta), \gamma(\theta)$ and the optimal frequency domain specifications $GM(\theta), PM(\theta)$ as functions of θ (See Table 1)
v. Express the controller in (17) in terms of time delay using functions $K_d(\theta), \gamma(\theta)$ by optimal strategy to select the frequency domain specifications $GM(\theta), PM(\theta)$
vi. Design the delay-dependent controller using Eq. (25).

4. Performance analysis on power system with nonreheated turbine having communication delay

In this section, performance analysis is made on the single area PS-NRT having communication delay whose nominal parameters are given in [4–6]. The higher-order single-area PS dynamics are modeled by a single fractional order pole model whose parameters are given in (**??**). Using the model parameters, the proposed controller in (25) is found as

$$C_{proposed}(s) = 6.617 K_d(\theta) s^{1.324 - \gamma(\theta)} \left(1 + \frac{1}{0.313 s^{1.324}}\right) \tag{27}$$

Here, $K(\theta)$ and $\gamma(\theta)$ are the gain and fractional order of D_BTF, and their functions can be seen in Table **??** based on three performance criteria; namely ISE, $ITSE$, and IAE. To be able to implement the proposed controller, communication delay must be estimated. This estimated communication delay is added to the time delay induced by the higher-order plant dynamics, which is equal to 0.249 s as seen in Eq. (**??**). After the communication delay is added to the induced time delay, the delay-dependent controller parameters can easily be calculated. In this study, a fixed communication delay of 2.28 s has been taken in the nominal system [4–6]. In the perturbed system, the other parameters of the power system have been modified by keeping the fixed communication delay constant at 2.28 s in the first scenario. In the second scenario, the communication delay is varied from 2.28 to 4 s.

The suggested LFC design methodology is contrasted with two alternative controller design methodologies relying on the identical frequency domain specifications [4, 5] using the same parameters of single area PS-NRT. The controllers proposed by the studies in [4, 5] are respectively as follows:

$$C_1(s) = 0.55 + \frac{0.55}{s} \tag{28}$$

$$C_2(s) = 0.29 + \frac{0.109}{s} \tag{29}$$

In addition to the comparison with integer-order PI controllers, the proposed controller is also compared with the fractional order PI controller designed using the same parameters of single area PS in [6], which is given as

$$C_3(s) = 0.2 + \frac{0.4}{s^{0.8}} \tag{30}$$

4.1. Analysis on nominal system

The load increment $\Delta P_d = 0.1$ p.u. at $t = 1$ s is applied to the designed control systems to test the disturbance rejection performances of all the controllers. The frequency change Δf responses which correspond to each control system are shown in Figure **??**. The disturbance rejection responses of the proposed three controllers are nonoscillatory compared to integer-order PI controller $C_1(s)$ and faster in comparison to integer-order PI controller $C_2(s)$. On the other hand, fractional-order PI controller $C_3(s)$ possesses a similar performance as the proposed controllers. Furthermore, Table **??** gives a numerical comparison of the disturbance rejection performances of all the controllers using three time domain criteria; namely, ISE, $ITSE$ and IAE. It can easily be said that the three proposed controllers outperform the other existing controllers in the literature in terms of the three performance criteria. Each of the three proposed controllers is the best according to the performance criterion on which its design is made. To be precise, the performance index values of the ISE, ITSE, and IAE based proposed controllers are 0.823×10^{-4}, 0.282×10^{-3}, and 2.587×10^{-2}, respectively. These values are shown in bold in Table **??**. Notably, the proposed controllers based on IAE and ITSE exhibit an enhancement in performance index by a minimum of 25%.

4.2. Analysis on perturbed system

Another critical issue in PS is that the designed control system must be robust against modeling errors. In this respect, we consider two cases to assess the robust performances of controllers. In the first case, all the plant parameters of PS-NRT are simultaneously changed by $\pm 10\%$ from their nominal values. Secondly, communication delay has been changed from $L = 2.28$ s to $L = 4$ s similar to the study in [5] .

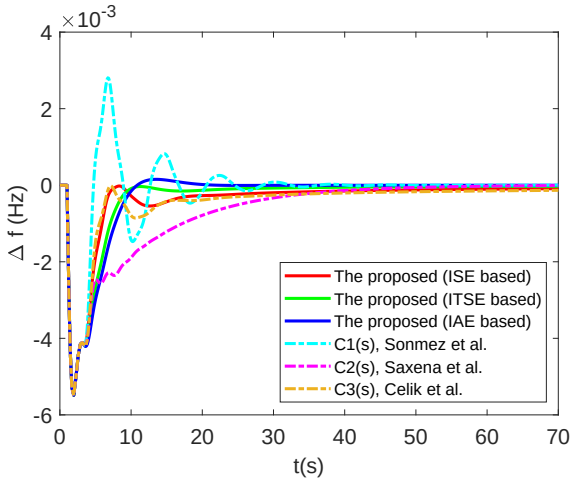

Figure 6. The disturbance rejection responses of all controllers using the parameters of nominal PS-NRT having communication delay.

Table 2. Performance index values for control systems on nominal systems and perturbed systems.

PI	Sonmez et al.	Saxena et al.	Celik et al.	Proposed (ISE based)	Proposed (ITSE based)	Proposed (IAE based)
Using nominal system						
ISE	2.402×10^{-4}	1.145×10^{-4}	0.853×10^{-4}	$\mathbf{0.823 \times 10^{-4}}$	0.878×10^{-4}	0.940×10^{-4}
ITSE	3.341×10^{-3}	0.588×10^{-3}	0.377×10^{-4}	0.308×10^{-3}	$\mathbf{0.282 \times 10^{-3}}$	0.315×10^{-3}
IAE	9.965×10^{-2}	4.373×10^{-2}	3.693×10^{-2}	3.249×10^{-2}	2.654×10^{-2}	$\mathbf{2.587 \times 10^{-2}}$
Using perturbed system (Case I)						
ISE (-10%)	0.766×10^{-4}	1.117×10^{-4}	0.716×10^{-4}	$\mathbf{0.691 \times 10^{-4}}$	0.761×10^{-4}	0.817×10^{-4}
ITSE (-10%)	3.058×10^{-4}	6.885×10^{-4}	3.470×10^{-4}	2.696×10^{-4}	$\mathbf{2.482 \times 10^{-4}}$	2.739×10^{-4}
IAE (-10%)	2.783×10^{-2}	4.854×10^{-2}	3.686×10^{-2}	3.122×10^{-2}	2.546×10^{-2}	$\mathbf{2.376 \times 10^{-2}}$
ISE ($+10\%$)	Unstable	1.184×10^{-4}	1.185×10^{-4}	1.094×10^{-4}	$\mathbf{1.067 \times 10^{-4}}$	1.126×10^{-4}
ITSE ($+10\%$)	Unstable	5.251×10^{-4}	6.311×10^{-4}	4.946×10^{-4}	$\mathbf{3.861 \times 10^{-4}}$	4.172×10^{-4}
IAE ($+10\%$)	Unstable	3.975×10^{-2}	4.998×10^{-2}	4.209×10^{-2}	3.235×10^{-2}	$\mathbf{3.112 \times 10^{-2}}$
Using perturbed system (Case II)						
ISE	Unstable	1.388×10^{-4}	1.388×10^{-4}	$\mathbf{1.352 \times 10^{-4}}$	1.457×10^{-4}	1.552×10^{-4}
ITSE	Unstable	$\mathbf{0.659 \times 10^{-3}}$	1.388×10^{-4}	0.705×10^{-3}	0.669×10^{-3}	0.749×10^{-3}
IAE	Unstable	4.371×10^{-2}	1.388×10^{-4}	4.978×10^{-2}	$\mathbf{4.315 \times 10^{-2}}$	4.332×10^{-2}
Using nominal system with GDB and GRC						
ISE	4.079×10^{-4}	2.076×10^{-4}	1.534×10^{-4}	$\mathbf{1.477 \times 10^{-4}}$	1.582×10^{-4}	1.698×10^{-4}
ITSE	5.252×10^{-3}	1.105×10^{-3}	0.781×10^{-3}	0.599×10^{-3}	$\mathbf{0.533 \times 10^{-3}}$	0.593×10^{-3}
IAE	12.29×10^{-2}	5.945×10^{-2}	5.569×10^{-2}	4.717×10^{-2}	3.692×10^{-2}	$\mathbf{3.514 \times 10^{-2}}$

Case I: Robustness to the plant parameter variation

The load increment $\Delta P_d = 0.1$ p.u. at $t = 1$ s is applied to the designed control systems to test the robustness of all the controllers using perturbed PS with -10% and $+10\%$ variations in the plant parameters. The frequency change Δf responses for two variations are illustrated in Figures 7a and 7b. The proposed controllers suppress the disturbance faster and with less oscillation in both cases. Integer-order PI controller $C_1(s)$ produces much smoother response, whereas integer-order PI controller $C_2(s)$ destabilizes the frequency fluctuation against $+10\%$ parameter variations. On the other hand, fractional-order PI controller $C_3(s)$

performs close to the proposed ISE based controller in both variations. These results are verified numerically in Table 2 using three-time domain criteria; namely, ISE, $ITSE$ and IAE. The best values are shown in bold in the table. From the table, the reason that the proposed $ITSE$ based controller has the best ISE value in case of $+10\%$ parameter variations is modeling error. Furthermore, similar to the nominal case, it is noteworthy to emphasize that the proposed IAE and ITSE based controller enhance the performance index by no less than 15% when subjected to parameter perturbations within the range of $\pm 10\%$.

Case II: Robustness to communication delay variation

When communication delay is varied from 2.28 to 4 s similar to the study in [5], the frequency change responses for load increment $\Delta P_d = 0.1$ p.u. at $t = 1$ sec are illustrated in Figure 7c. The proposed $ITSE$ and IAE based delay-dependent controllers suppress the disturbance faster and the proposed ISE based delay-dependent controller possesses slightly oscillatory performance in comparison to integer-order PI controller $C_2(s)$. On the other hand, integer-order PI controller $C_1(s)$ gives an unstable response while fractional order PI controller $C_3(s)$ has a highly oscillatory performance compared to the proposed controllers. Moreover, the corresponding time domain criteria values of all the designed controllers can be seen in Table 2. It is evident that the performance index values of the proposed controller and integer-order PI controller $C_2(s)$ are quite similar. To be specific, the controllers proposed in this study slightly outperform in terms of ISE and $ITSE$ criteria.

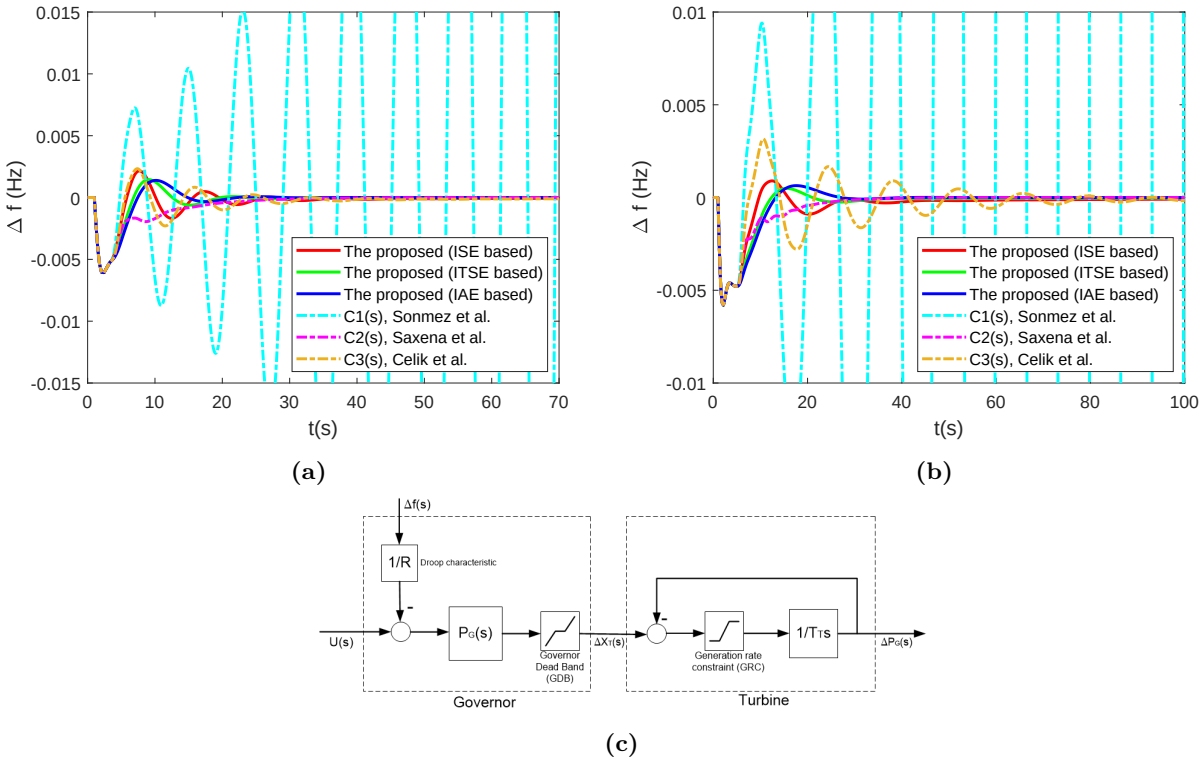

Figure 7. The disturbance rejection responses of all designed controllers using (a) perturbed system (Case I - $+10\%$), (b) perturbed system (Case I - -10%), and (c) perturbed system (Case II)

4.3. Analysis on nominal system with governor dead band and generator rate constraint nonlinearities

In practice, PS needs to manage physical nonlinear constraints like governor dead band (GDB) and generator rate constraint (GRC), etc. These nonlinear constraints are illustrated in Figure 8a. In performance analysis, GDB and GRC are taken as 0.036 Hz and 0.1 p.u. MW/min. respectively. Moreover, the load increment $\Delta P_d = 0.1$ p.u. at $t = 1$ s is applied to the power system with GDB and GRC nonlinearities to test the disturbance rejection performances of all the controllers. The frequency change Δf responses which correspond to each control system are depicted in Figure 8b. Similar to the nominal case, the disturbance rejection responses of the proposed three controllers are nonoscillatory and faster than integer-order PI controllers, $C_1(s), C_2(s)$, and possess a similar performance as fractional-order PI controller $C_3(s)$. Moreover, Table 2 gives a numerical comparison of the disturbance rejection performances of all the controllers using three-time domain criteria; namely, ISE, $ITSE$ and IAE. All the values in the table are approximately two-fold higher compared to the nominal case. It can easily be observed that the three proposed controllers are superior to the other existing controllers in the literature in terms of the three performance criteria. Moreover, each of the three proposed controllers is the best according to the performance criterion on which its design is made. Their best values are shown in bold in Table 2. It is noteworthy to emphasize that the proposed IAE and ITSE based controller enhances the performance index by no less than 30% when subjected to governor dead band and generator rate constraint nonlinearities.

4.4. Analysis on multiarea case using nominal systems

In this section, the single area PS-NRT is extended to the two-area interconnected power system illustrated in Figure 9a. The power system parameters in the first and second areas are taken as equal to each other, and the parameters given in Section 2.1 are utilized in the simulation. Moreover, the additional parameters are taken as the ratio between the base values of two areas $a_{12} = -1$ and tie line exchange power $T_{12} = 0.545 puMW$ [16] The primary control objective of the stable power system is to minimize the system frequency deviation within the two designated areas: Δf_1 in area 1, Δf_2 in area 2. Additionally, the aim is to limit the deviation in the tie line power flow denoted as ΔP_{tie} between the two areas when subjected to the load disturbances ΔP_{D1} and ΔP_{D2} in their respective areas. Given that the system parameters are identical for both areas and the deviation in P_{tie} is a direct result of the difference $\Delta f_1 - \Delta f_2$, the performance of the system can be primarily assessed by introducing a disturbance ΔP_{D1} into the system and monitoring the time response of Δf_1. The simulations are done by applying a single step disturbance of $\Delta P_{D1} = 0.01 pu$ to the first area. Then, the frequency deviation of the first area, the frequency deviation of the second area and the deviation of P_{tie} for the proposed controllers are shown in Figures 9b, 9c, and 9d respectively. The proposed controllers have performed satisfactorily in the two area interconnected power system.

5. Conclusion

In this paper, a fractional delay-dependent LFC design methodology for a single-area PS-NRT with communication delay is proposed based on GPM specifications. In this methodology, the closed-loop reference transfer function relies on D_BTF. GPM specifications are established in order to optimize the reference model based on three time-domain performance indices, i.e. ISE, IAE, and ITSE. Moreover, the single-area PS-NRT with communication delay is represented by a class of fractional-order model. Using the fractional-order model and the optimal closed-loop reference model, the controller parameters are determined and then updated via the communication delay variation.

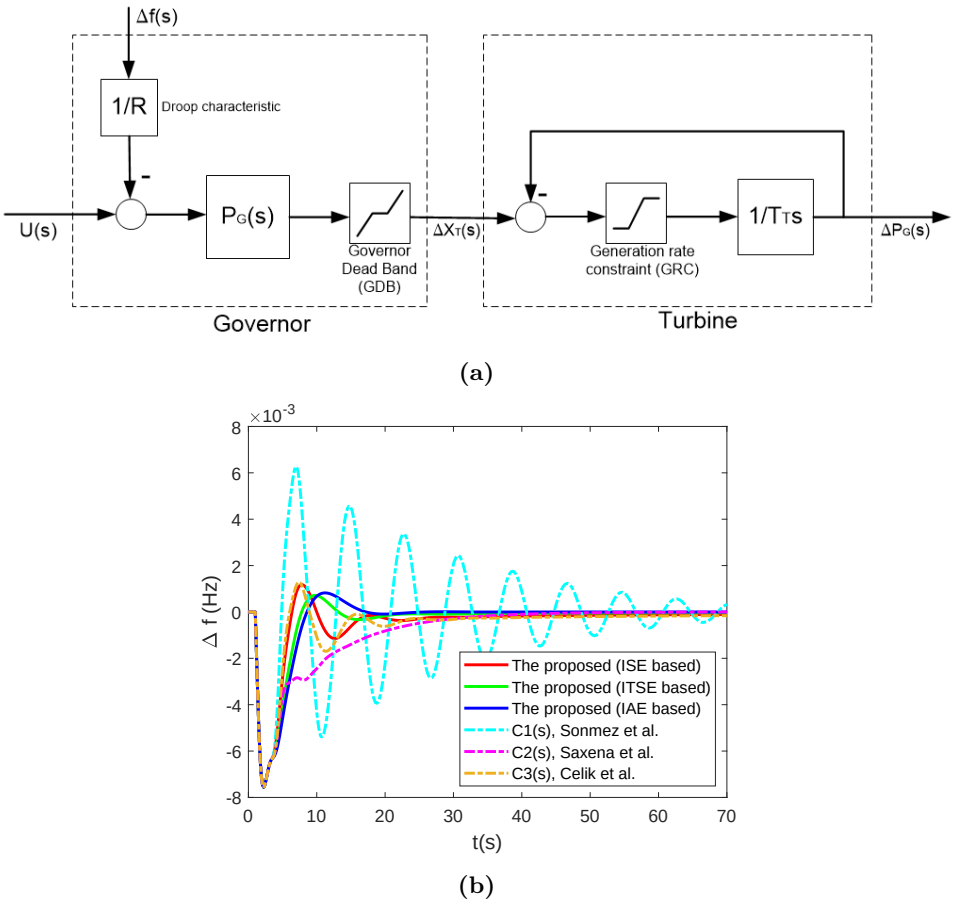

Figure 8. (a) The block diagram of governor with GDB and turbine with GRC and (b) The disturbance rejection responses of all designed controllers using nominal system with GRC and GDB.

The proposed controllers are implemented in a single area PS-NRT having communication delay, and are compared with other controllers designed relying on the identical frequency domain specifications. The performance analysis of the proposed methodology is made against communication delay or model parameter variations, nonlinearities, i.e. governer dead band and governor rate constraints. The results on nominal PS with/without GDB and GRC and perturbed power systems show that the proposed controllers suppress the disturbance faster and with less oscillation in comparison to integer order PI controllers. On the other hand, although fractional-order PI controller possesses a similar performance as the proposed controllers, it has a highly oscillatory performance against communication delay changes. It can be said that the proposed delay-dependent controllers are more robust to communication delay changes as well as system model parameter variations. Moreover, the three proposed controllers considerably outperform according to the three performance criteria; namely, ISE, ITSE and IAE. On the other hand, the proposed controllers have performed satisfactorily in the two area interconnected power system.

The future study will focus on the application of the proposed control design approach to different types of multi-area PS. Moreover, the proposed methodology can be applied to power systems with reheated or hydro turbines instead of PS-NRT.

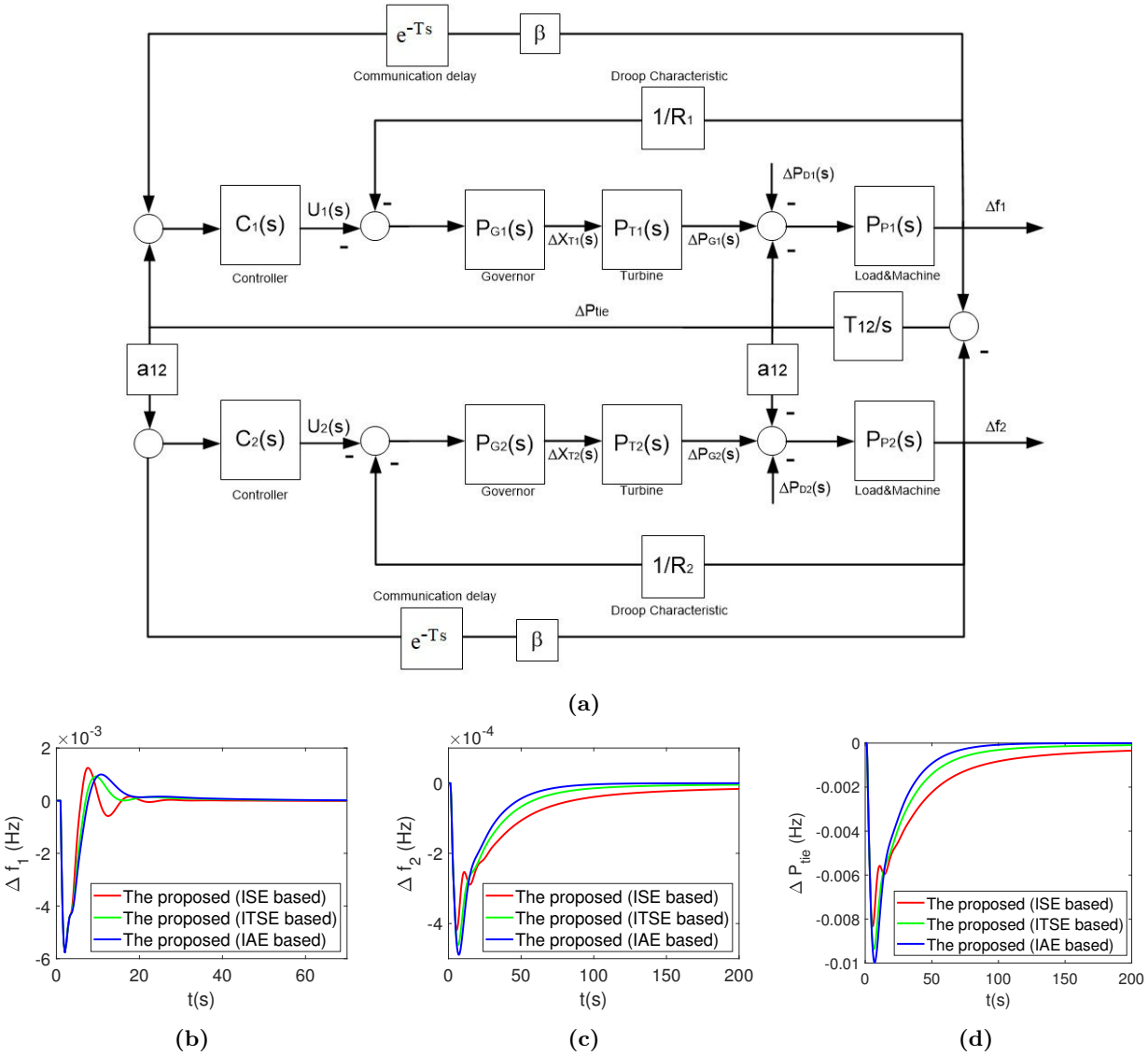

Figure 9. (a) Block diagram of multi area power system, (b) The frequency deviation of the first area, (c) The frequency deviation of the second area, and (d) The deviation of P_{tie}.

References

[1] Tan W. Tuning of PID load frequency controller for power systems. Energy Conversion and Management. 2009;50 (6):1465-72.

[2] Saxena S, Hote YV. Load frequency control in power systems via internal model control scheme and model-order reduction. IEEE transactions on power systems. 2013;28 (3):2749-57.

[3] Mishra AK, Mishra P, Mathur H. A deep learning assisted adaptive nonlinear deloading strategy for wind turbine generator integrated with an interconnected power system for enhanced load frequency control. Electric Power Systems Research. 2023;214:108960.

[4] Sönmez S, Ayasun S. Stability region in the parameter space of PI controller for a single-area load frequency control system with time delay. IEEE Transactions on Power Systems. 2015;31 (1):829-30.

[5] Saxena S, Hote YV. PI controller based load frequency control approach for single-area power system having communication delay. IFAC-PapersOnLine. 2018;51 (4):622-6.

[6] Çelik V, Özdemir MT, Lee KY. Effects of fractional-order PI controller on delay margin in single-area delayed load frequency control systems. Journal of Modern Power Systems and Clean Energy. 2019;7 (2):380-9.

[7] Das S, Saha S, Das S, Gupta A. On the selection of tuning methodology of FOPID controllers for the control of higher order processes. ISA transactions. 2011;50 (3):376-88.

[8] Yumuk E, Güzelkaya M, Eksin İ. A Robust Fractional-Order Controller Design with Gain and Phase Margin Specifications based on Delayed Bode's Ideal Transfer Function. Journal of the Franklin Institute. 2022;359 (11):5341-53.

[9] Mohamed TH, Alamin MAM, Hassan AM. A novel adaptive load frequency control in single and interconnected power systems. Ain Shams Engineering Journal. 2021;12 (2):1763-73.

[10] Saxena S. Load frequency control strategy via fractional-order controller and reduced-order modeling. International Journal of Electrical Power & Energy Systems. 2019;104:603-14.

[11] Zhuo-Yun N, Yi-Min Z, Qing-Guo W, Rui-Juan L, Lei-Jun X. Fractional-order PID controller design for time-delay systems based on modified bodeâ€™s ideal transfer function. IEEE Access. 2020;8:103500-10.

[12] Yumuk E, Güzelkaya M, Eksin I. Application of fractional order PI controllers on a magnetic levitation system. Turkish Journal of Electrical Engineering & Computer Sciences. 2021;29 (1):98-109.

[13] Yumuk E, Güzelkaya M, Eksin İ. Fractional-Order Controller Design via Optimal Selection Strategy of Frequency-domain Specifications. International Journal of Systems Science. 2023;54 (10):2239-52.

[14] Zhang L, Hu X, Wang Z, Sun F, Dorrell DG. Fractional-order modeling and State-of-Charge estimation for ultracapacitors. Journal of Power Sources. 2016;314:28-34.

[15] Grabowski D, Jakubowska-Ciszek A, Klimas M. Fractional-Order Model of Electric Arc Furnace. IEEE Transactions on Power Delivery. 2023.

[16] Yeşil E, Güzelkaya M, Eksin İ. Self tuning fuzzy PID type load and frequency controller. Energy Conversion and Management. 2004;45 (3):377-90.